Chemical microanalysis of rare-earth–transition metal–boron alloys and magnets using scanning electron microscopy

R.N. Faria*, H. Takiishi, A.R. M. Castro, L.F.C.P. Lima, I. Costa

Instituto de Pesquisas Energéticas e Nucleares IPEN-CNEN, CEP 05422-970, São Paulo-SP, Brazil

Abstract

This paper reports the results of investigations of chemical microanalyses of various alloys and sintered magnets with well-known compositions. Analyses of neodymium, praseodymium, iron, cobalt, niobium and copper have been carried out using energy-dispersive X-ray spectrometry. Quantitative analyses of boron have been carried out using wavelength-dispersive X-ray spectrometry. The resulting mean values were compared with data reported in the literature for the various phases present in these magnetic materials. © 2002 Elsevier Science B.V. All rights reserved.

Keywords: Permanent magnets; Alloys; SEM; EDX; WDX

1. Introduction

Quantitative light element microanalysis of Nd–Fe–B alloys and magnets has been carried out employing wavelength-dispersive X-ray spectrometry (WDX) [1–4]. Energy-dispersive X-ray spectrometry (EDX) is more widely used to analyze alloys and magnets containing rare earth (RE) and transition metal (TM) [5–17]. Boron and oxygen, however, cannot be analyzed by EDX and the ratio TM:RE has been used to identify the phase under investigation [18–20]. For boron and oxygen-free phases, or phases containing only small amount of these elements, the identification is readily accomplished. Conversely, phases with a higher amount of boron or oxygen can be somewhat more difficult to be identified by EDX since the amount of these elements is unevenly distrib-

uted in the measured RE and TM contents. In the present work an assessment of EDX as a method of characterizing phases in RE–TM–B-based alloys and magnets has been carried out. For a comparison, various cast alloys and magnets have been analyzed in this work by EDX combined with WDX and also using only EDX. Five main phases have been investigated, namely, the $RE_2TM_{14}B$ matrix phase (ϕ), the grain boundary RE-rich phase (RE-rich), the boron-rich phase (η), the TM-rich phase (α-TM) and the RE_2TM_{17} phase. The compositions studied in this investigation were chosen to complement various works found in the literature.

2. Experimental

Various commercial alloys were investigated in the as-cast and vacuum-annealed states (1000°C

---

*Corresponding author.

E-mail address: rfaria@net.ipen.br (R.N. Faria).

for 24 h). Permanent magnets were prepared using the hydrogen decrepitation (HD) process [21,22]. The microstructures of the specimens were examined using an optical microscope and a scanning electron microscope (SEM) with energy- and wavelength-dispersive X-ray analysis facilities (WDX + EDX). Microanalyses were also performed using an SEM fitted only with EDX. Average data were obtained from five independent measurements from each phase.

3. Results and discussion

Chemical compositions of the matrix phase measured by EDX + WDX on an SEM are listed in Table 1. Literature results used for comparison are an average of several measurements. The relative atomic ratio TM:RE for the matrix phase is also shown in Table 1. Compositions determined in the centers of the hard magnetic matrix phase exhibited values as low as 11.4 at% and as high as 12.9 at%. The mean value of the atomic ratio TM:RE was 6.7, which is just below the expected value. In general, deviations from the stoichiome-

try for RE were for higher values than 11.8 at% and lower values than 82.3 at% for TM. Rather surprisingly, some quite high values for boron (>6 at%) were measured in this work and also in Refs. [1,3]. Fig. 1 shows the relative frequency of RE-measured composition on the analyzed matrix phase. Gaussian mean value was 11.9 at%, which
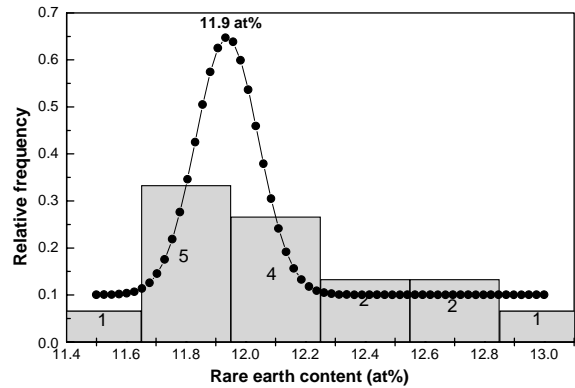

Fig. 1. Relative frequency of measured composition of RE content on the matrix phase measured using EDX + WDX (Table 1).

Table 1
Neodymium, iron and boron contents of the matrix phase analyzed by EDX + WDX (stoichiometry: $RE_{11.8}TM_{82.3}B_{5.9}$ or $RE_2TM_{14}B$)

Alloy or magnet composition (at%)	Measured concentration (at%)			TM:RE ratio	Deviation from stoichiometry (at%)			Ref.
	RE	TM	B		δRE	δTM	δB	
$Nd_{11.77}Fe_{80.35}B_{5.88}Nb_{2.0}$ alloy	12.1	79.8	7.6	**6.6**	0.3	−2.5	1.7	[3]
$Nd_{11.77}Fe_{80.35}B_{5.88}Nb_{2.0}$-annealed alloy	11.9	81.4	6.4	**6.8**	0.1	−0.9	0.5	[3]
$Nd_{11.77}Fe_{80.35}B_{5.88}Nb_{2.0}$ magnet	12.0	81.1	6.7	**6.8**	0.2	−1.2	0.8	[3]
$Nd_{15}Fe_{77}B_8$ alloy (B standard, COR-2)	10.6	82.6	5.8	**7.8**	−1.2	0.3	−0.1	[1]
$Nd_{15}Fe_{77}B_8$ alloy (B standard, ZAF-4)	11.4	79.3	7.8	**7.0**	−0.4	−3.0	1.9	[1]
$Nd_{15}Fe_{77}B_8$ alloy (FeB standard, ZAF-4)	11.9	80.8	5.8	**6.8**	0.1	−1.5	−0.1	[1]
$Nd_{16}Fe_{76}B_8$ magnet (FeB, ZAF-4)	12.8	79.2	6.3	**6.2**	1.0	−3.1	0.4	[1]
$Nd_{16.4}Fe_{75.7}B_{7.9}$ magnet	11.7	81.9	5.1	**7.0**	−0.1	−0.4	−0.8	[4]
$Nd_{16.4}Fe_{75.7}B_{7.9}$ magnet treated	12.1	79.7	7.5	**6.6**	0.3	−2.6	−1.6	[4]
$Nd_{17}Fe_{76.5}B_5Cu_{1.5}$ magnet	11.9	82.3	5.8	**6.9**	0.1	0.0	−0.1	[2]
$Pr_{17}Fe_{76.5}B_5Cu_{1.5}$ alloy	12.4	81.1	6.5	**6.5**	0.6	−1.2	0.6	This work
$Pr_{17}Fe_{76.5}B_5Cu_{1.5}$ magnet	12.9	81.7	5.4	**6.3**	1.1	−0.6	−0.5	This work
$Pr_{17}Fe_{73.5}B_8Cu_{1.5}$-annealed alloy	12.7	79.5	7.8	**6.3**	0.9	−2.8	1.9	This work
$Pr_{17}Fe_{73.5}B_8Cu_{1.5}$ heat-treated magnet	12.2	80.6	7.2	**6.6**	0.4	−1.7	1.3	This work
$Pr_{20}Fe_{74}B_4Cu_2$ alloy	12.5	80.3	7.2	**6.4**	0.7	−2.0	1.3	This work
$Pr_{20}Fe_{74}B_4Cu_2$-annealed alloy	11.9	81.8	6.3	**6.9**	0.1	−0.5	0.4	This work

Oxygen was also analyzed in Refs. [1,4] and niobium in Ref. [3].

is closer to the expected stoichiometric value of 11.8 at%. Bearing in mind that the 15 measurements presented in Fig. 1 are the average of several individual readings, an excellent agreement between the theoretical and the measured mean values for RE content of the matrix phase has been obtained.

Chemical compositions of the matrix phase measured by EDX on an SEM are listed in Table 2. Again, various results obtained from literature for comparison are an average of several measurements. The relative atomic ratio TM:RE for the matrix phase are also shown in Table 2. Compositions determined in the centers of the hard

Table 2

Neodymium, praseodymium, cobalt and iron contents analyzed by EDX for the matrix phase

Alloy or magnet composition (at%) and condition	Measured concentration (at%)		TM:RE ratio	Deviation from stoichiometry (at%)		Ref.
	RE	TM		δRE	δTM	
$Nd_2Fe_{8.4}Co_{5.6}B$-annealed alloy	12.4	87.7	**7.1**	0.6	5.4	[17]
$Nd_{12.8}Fe_{79.8}B_{7.4}$ magnet	12.2	87.8	**7.2**	0.4	5.5	[16]
$Nd_{13.7}(Fe_{63.5}Co_{16.7})B_6Zr_{0.1}$ alloy	14.3	85.7	**6.0**	2.5	3.4	[9]
$Nd_{13.7}(Fe_{63.5}Co_{16.7})B_6Zr_{0.1}$-annealed alloy	14.2	85.8	**6.0**	2.4	3.5	[9]
$Pr_{13.7}(Fe_{63.5}Co_{16.7})B_6Zr_{0.1}$ alloy	14.7	85.3	**5.8**	2.9	3.0	[9]
$Pr_{13.7}(Fe_{63.5}Co_{16.7})B_6Zr_{0.1}$-annealed alloy	14.5	85.5	**5.9**	2.7	3.2	[9]
$Nd_{15}Fe_{77}B_8$ alloy 1	14.0	86.0	**6.1**	2.2	3.7	This work
$Nd_{15}Fe_{77}B_8$ alloy 2	13.0	87.0	**6.7**	1.2	4.7	This work
$Nd_{15}Fe_{77}B_8$ alloy	12.6	87.4	**6.9**	0.8	5.1	[10]
$Nd_{15}(Fe_{57}Co_{20})B_8$ alloy	12.4	87.6	**7.1**	0.6	5.3	[10]
$Nd_{15}Co_{77}B_8$ alloy	12.5	87.5	**7.0**	0.7	5.2	[10]
$Nd_{15}(Fe_{69.3}Co_{7.7})B_8$ alloy	12.3	87.7	**7.1**	0.5	5.4	[5]
$Nd_{15}(Fe_{61.6}Co_{15.4})B_8$ alloy	12.7	87.3	**6.9**	0.9	5.0	[5]
$Nd_{15}(Fe_{53.9}Co_{23.1})B_8$ alloy	12.5	87.5	**7.0**	0.7	5.2	[5]
$Nd_{15}(Fe_{38.5}Co_{38.5})B_8$ alloy	12.4	87.6	**7.1**	0.6	5.3	[5]
$Nd_{15}(Fe_{38.5}Co_{38.5})B_8$ alloy	13.0	87.0	**6.7**	1.2	4.7	[5]
$Nd_{15}(Fe_{73}Co_{3.5})B_8Cu_{0.5}$ alloy	14.2	86.6	**6.1**	2.4	4.3	[6]
$Nd_{15}(Fe_{73}Co_{3.5})B_8Nb_{0.5}$ alloy	14.9	85.1	**5.7**	3.1	2.8	[6]
$Nd_{15.2}(Fe_{72.2}Co_5)B_{7.6}$ magnet	13	87	**6.7**	1.2	4.7	[7]
$(Nd_{13.5}Dy_{1.5})Fe_{78}B_7$ magnet	12.7	87.3	**6.9**	0.9	5.0	[12]
$(Nd_{13.5}Dy_{1.5})(Fe_{68}Co_{10})B_7$ magnet	12.8	87.2	**6.8**	1.0	4.9	[12]
$Nd_{15}Fe_{77}B_6$ magnet	13.4	86.6	**6.5**	1.6	4.3	[10]
$Nd_{15}(Fe_{bal}Co_{30})B_{5.5}Al_4$ magnet	13.6	86.4	**6.4**	1.8	4.1	[13]
$Pr_{16}Fe_{76}B_8$ magnet	13.0	87.0	**6.7**	1.2	4.7	This work
$Pr_{16}Fe_{76}B_8$ heat-treated magnet	13.0	87.0	**6.7**	1.2	4.7	This work
$Nd_{16}Fe_{76}B_8$ magnet	14.5	85.5	**5.9**	2.7	3.2	[14]
$Nd_{16}Fe_{76}B_8$ (Al) magnet	13.2	85.6	**6.5**	1.4	3.3	[15]
$Nd_{16}Fe_{76}B_8$ (Al) heat-treated magnet	13.4	85.3	**6.4**	1.6	3.0	[15]
$(Nd_{14.4}Dy_{1.6})(Fe_{67}Co_5V_4)B_8$ alloy	13.3	86.7	**6.5**	1.5	4.4	[8]
$(Nd_{14.4}Dy_{1.6})(Fe_{67}Co_5V_4)B_8$ magnet	13.3	86.7	**6.5**	1.5	4.4	[8]
$(Nd_{14.5}Dy_{1.5})Fe_{76}B_7Nb_1$ alloy	10.8	89.2	**8.3**	−1.0	6.9	This work
$(Nd_{14.5}Dy_{1.5})Fe_{76}B_7Nb_1$ magnet	11.7	88.3	**7.5**	−0.1	6.0	This work
$Nd_{17}(Fe_{0.7}Co_{0.3})_{77}B_8$ magnet	13.6	86.4	**6.4**	1.8	4.1	This work
$Nd_{17}Fe_{76.5}B_5Cu_{1.5}$ magnet	13.0	87.0	**6.7**	1.2	4.7	This work
$Pr_{20}Fe_{74}B_4Cu_2$ magnet	14.2	85.8	**6.0**	2.4	3.5	This work
$Pr_{20}Fe_{74}B_4Cu_2$ heat-treated magnet	14.7	85.3	**5.8**	2.9	3.0	This work
$Pr_{20}Fe_{74}B_4Cu_2$ alloy	16.5	83.5	**5.1**	4.7	1.2	This work
$Pr_{20}Fe_{74}B_4Cu_2$-annealed alloy	15.9	84.1	**5.3**	4.1	1.8	This work

Zirconium was analyzed in Ref. [9] (<1 at%) and aluminum in Ref. [15] (1.2–1.3 at%).

magnetic matrix phase exhibited values as low as 10.8 at% and as high as 16.5 at%. A wide range of atomic ratio TM:RE was found for the matrix phase measured without analyzing the boron content. Fig. 2 shows the relative frequency of EDX-measured composition of RE on the matrix phase. Gaussian mean value was 13.0 at%, which is 1.2 at% higher than the stoichiometric value and scatter is more pronounced in this case. Deviation of RE and TM from the stoichiometry versus the TM:RE ratio for the matrix phase measured with

EDX is shown in Fig. 3. Measurement deviation in the RE content is minimized for ratios around 7.0–7.5, and in this case the disparity from stoichiometry, caused by not measuring boron content, is concentrated on the TM content. Fig. 4 shows the variation of the ratio TM:RE with the analyzed RE content on the matrix phase. The stoichiometric point with a ratio of 7 and the RE content of 11.8 at% was plotted as a reference. Discrepancy from the true value is minimized in both techniques when the ratio TM:RE is closer to 7 and the measured rare earth content is around 12 at%. The microstructure of an as-cast ingot of
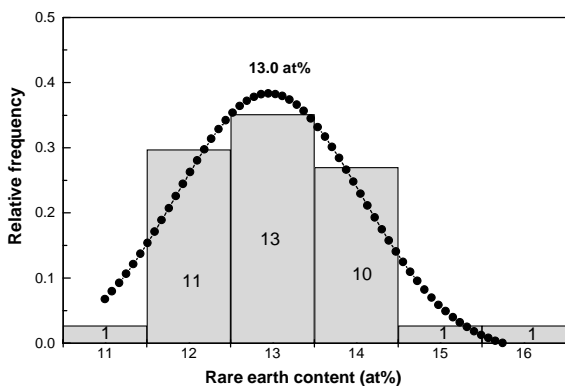

Fig. 2. Relative frequency of measured composition of RE content on the matrix phase measured using EDX (Table 2).
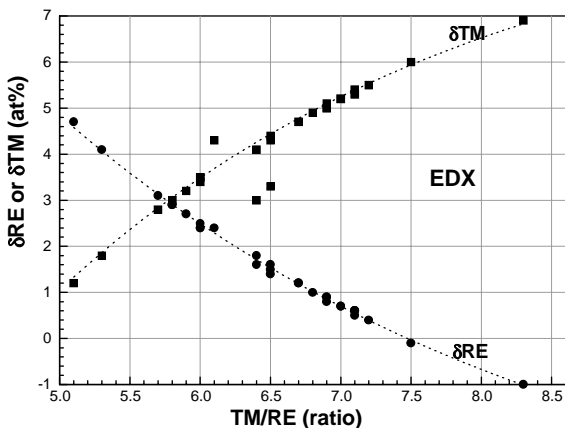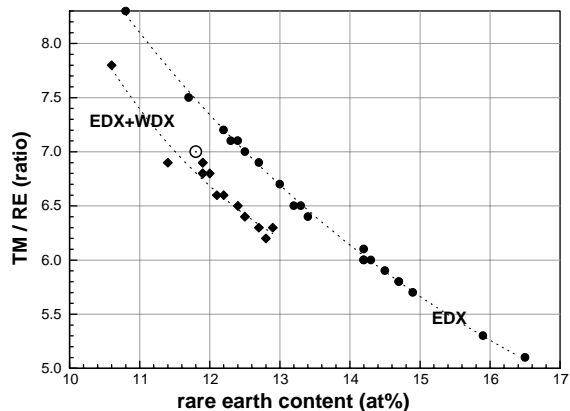

Fig. 3. Variation of the deviation of RE and TM from the stoichiometry with the ratio TM:RE for the matrix phase without measuring boron concentration.

Fig. 4. Variation of TM:RE ratio with the RE content analyzed on the matrix phase.
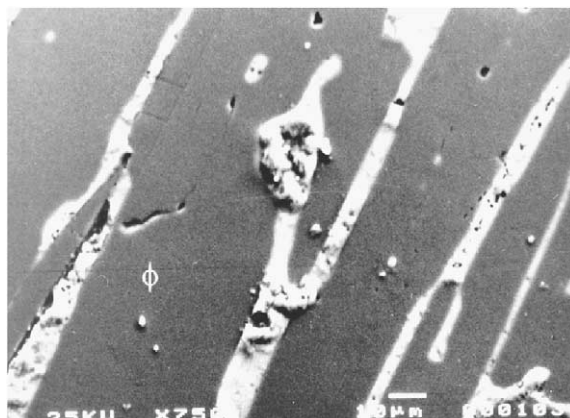
Fig. 5. Microstructure of the $Nd_{16}Fe_{76}B_8$ alloy showing the matrix phase. ($750 \times$, $10 \mu m$).

the $Nd_{16}Fe_{76}B_8$ alloy, with columnar grains of the matrix phase (gray), is shown in Fig. 5. Chemical compositions of the grain boundary phase or RE-rich phase are listed in Table 3 (white phase in Fig. 5). RE contents determined by EDX + WDX showed values around 94–96 at%. A wider range of values was measured using the EDX. Fig. 6 shows that the RE mean value of the RE-rich phase is around 93.9 at% (Gaussian fitting).

Magnetic domain patterns revealed by ferrofluid in an $Nd_{16}Fe_{76}B_8$ alloy are shown in Fig. 7. The columnar grains grow with their major axis predominantly in the basal plane rather than along the c-axis. The dark phase is the RE-rich
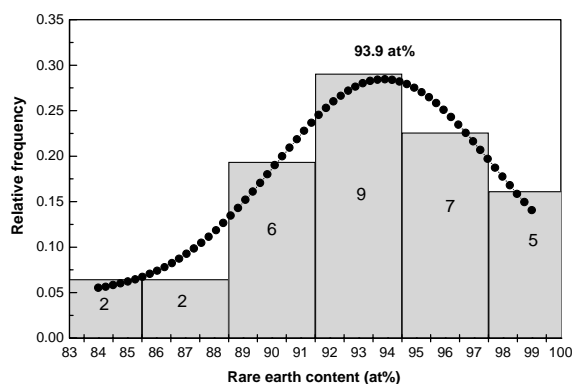

Fig. 6. Relative frequency of analyzed RE content on the grain boundary phase using EDX + WDX or only EDX (Table 3).

Table 3
Neodymium, praseodymium, cobalt, iron and copper contents analyzed by EDX and/or WDX for the RE-rich phase

Alloy or magnet composition (at%)	Measured concentration (at%)				Ref.
	RE	TM	B	O, Nb or Cu	
$Nd_{11.77}Fe_{80.35}B_{5.88}Nb_{2.0}$ alloy	94.7	1.4	3.7	0.13	[3]
$Nd_{15}Fe_{77}B_8$ alloy 1	94.0	6.0	—	—	This work
$Nd_{15}Fe_{77}B_8$ alloy 2	95.0	5.0	—	—	This work
$Nd_{15}Fe_{77}B_8$	96.5	3.4	—	—	[10]
$Nd_{15}Fe_{77}B_8$ (triple junction, B standard)	85.4	~1	<1	13.4	[1]
$Nd_{15}Fe_{77}B_8$ (grain boundary, B standard)	86.5	~1	<1	13.1	[1]
$Nd_{15}Fe_{77}B_8$ (triple junction, FeB standard)	85.4	~1	<1	13.4	[1]
$Nd_{15}Fe_{77}B_8$ (grain boundary, FeB standard)	85.5	~1	<1	14.0	[1]
$Nd_{15}Fe_{77}B_8$ (triple junction, COR-2)	90.4	~1	<1	8.7	[1]
$Nd_{15}Fe_{77}B_8$ (grain boundary, COR-2)	90.6	~1	<1	8.3	[1]
$Nd_{15}Fe_{77}B_8$ (using μ/ρ, Nd-Oxygen)	90.5	~1	<1	8.7	[1]
$Nd_{15}Fe_{77}B_8$ (using μ/ρ, Nd-Oxygen)	91.4	~1	<1	8.3	[1]
$Nd_{15}Fe_{77}B_8$ (using μ/ρ, Nd-Oxygen)	89.0	~1	<1	10.2	[1]
$Nd_{15}Fe_{77}B_8$ (using μ/ρ, Nd-Oxygen)	90.1	~1	<1	9.7	[1]
$(Nd_{13.5}Dy_{1.5})Fe_{78}B_7$ magnet	93.3	6.7	—	—	[12]
$Nd_{15.2}(Fe_{72.2}Co_5)B_{7.6}$	98	2	—	—	[7]
$Pr_{16}Fe_{76}B_8$ magnet	95.0	5	—	—	This work
$Pr_{16}Fe_{76}B_8$ heat-treated magnet	96.9	4	—	—	This work
$Nd_{16}Fe_{76}B_8$ (Al) magnet	96.2	3.8	—	—	[15]
$(Nd_{14.4}Dy_{1.6})(Fe_{67}Co_5V_4)B_8$ alloy	96.6	<3	—	—	[8]
$(Nd_{14.4}Dy_{1.6})(Fe_{67}Co_5V_4)B_8$ magnet	93.0	6	—	—	[8]
$Nd_{17}Fe_{76.5}B_5Cu_{1.5}$ magnet	93.0	6	—	<1	This work
$Pr_{17}Fe_{76.5}B_5Cu_{1.5}$ alloy	98.0	~2	<1	—	This work
$Pr_{17}Fe_{76.5}B_5Cu_{1.5}$-annealed alloy	99.0	~1	<1	—	This work
$Pr_{17}Fe_{76.5}B_5Cu_{1.5}$ magnet	95.0	~4	<1	—	This work
$Pr_{20}Fe_{74}B_4Cu_2$ alloy	99.0	~1	<1	—	This work
$Pr_{20}Fe_{74}B_4Cu_2$-annealed alloy	98.0	~2	<1	—	This work
$Pr_{20}Fe_{74}B_4Cu_2$ magnet	86.5	6.1	—	7.4	This work
$Pr_{20}Fe_{74}B_4Cu_2$ heat-treated magnet	93.7	6.0	—	<1	This work
$Pr_{20}Fe_{74}B_4Cu_2$ magnet 1	94.9	5.1	—	<1	This work
$Pr_{20}Fe_{74}B_4Cu_2$ heat-treated magnet 1	97.0	3.0	—	<1	This work

Oxygen was analyzed in Ref. [1], niobium in Ref. [3] and Al in Ref. [15].

phase and the light phase is the B-rich phase (or boride), and both are non-magnetic phases. In optical micrographs, it is difficult to distinguish boride from the matrix phase without ferrofluid or polarized light whilst the RE-rich phase is much darker. Identification of boride in SEM images is also difficult due to 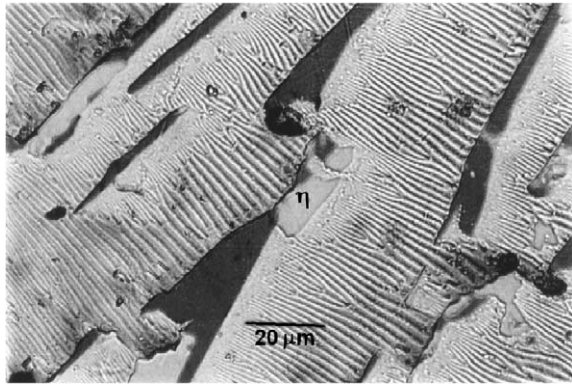similar contrasts of the matrix phase and the B-rich phase. Even back-scattered electron detection yields a poor contrast. EDX is carried out on areas surrounding the RE-rich phase in order to locate the boride by its distinct composition. Table 4 show the analyzed RE, TM and boron contents for the boron-rich phase. Boron concentration was measured by WDX in

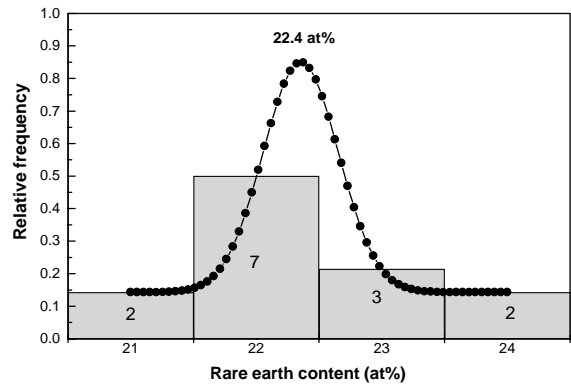Fig. 7. Micrograph showing the ϕ, η and RE-rich phases (ferrofluid).

Fig. 8. Relative frequency of measured composition of RE content on the boride using EDX (Table 4).

Table 4
Neodymium, praseodymium, cobalt and iron contents analyzed by EDX for the boron-rich phase (boride stoichiometry: $R_{12.1}M_{44}B_{44}$ or $R_{1+\varepsilon}M_4B_4$)

| Alloy or magnet composition (at%)	Measured concentration (at%)			TM:RE ratio	Deviation from stoichiometry (at%)			Ref.
	RE	TM	B		δRE	δTM	δB	
$Nd_{15}Fe_{77}B_8$ alloy	10.1	33.9	54.3	3.4	−2.0	−10.1	10.3	[1]
$Nd_{15}Fe_{77}B_8$ alloy	11.5	39.6	48.2	3.4	−0.6	−4.4	4.2	[1]
$Nd_{15}Fe_{77}B_8$ alloy	11.9	43.8	42.9	3.7	−0.2	−0.2	−1.1	[1]
$Nd_{15}Fe_{77}B_8$ alloy 1	23.0	77.0	—	3.3	10.9	33.0	—	This work
$Nd_{15}Fe_{77}B_8$ alloy 2	22.0	78.0	—	3.5	9.9	34.0	—	This work
$Nd_{15}Fe_{69.3}Co_{7.7}B_8$	21.9	78.1	—	3.6	9.8	34.1	—	[5]
$Nd_{15}(Fe_{61.6}Co_{15.4})B_8$ alloy	22.1	77.9	—	3.5	10.0	33.9	—	[5]
$Nd_{15}(Fe_{53.9}Co_{23.1})B_8$ alloy	22.2	77.8	—	3.5	10.1	33.8	—	[5]
$Nd_{15}(Fe_{69.3}Co_{7.7})B_8$ alloy	21.8	78.2	—	3.6	9.7	34.2	—	[5]
$Nd_{15}(Fe_{69.3}Co_{7.7})B_8$ alloy	22.0	78.0	—	3.5	9.9	34.0	—	[5]
$Nd_{15}(Fe_{73}Co_{3.5})B_8Cu_{0.5}$ alloy	24.6	75.4	—	3.1	12.5	31.4	—	[6]
$Nd_{15}(Fe_{73}Co_{3.5})B_8Nb_{0.5}$ alloy	24.2	75.8	—	3.1	12.1	31.8	—	[6]
$Nd_{15.2}(Fe_{72.2}Co_5)B_{7.6}$ magnet	22	78	—	3.5	9.9	34.0	—	[7]
$Nd_{16}Fe_{76}B_8$ (Al) magnet	23.6	76.4	—	3.2	11.5	32.4	—	[15]
$Nd_{16}Fe_{76}B_8$ (Al) magnet	22.5	77.5	—	3.4	10.4	33.5	—	[15]
$Pr_{16}Fe_{76}B_8$ magnet	21.0	79.0	—	3.8	8.9	35.0	—	This work
$Pr_{16}Fe_{76}B_8$ heat-treated magnet	22.0	78.0	—	3.5	9.9	34.0	—	This work
$Nd_{16.4}Fe_{75.7}B_{7.9}$ magnet treated	12.2	44	43.7	3.6	0.1	0.0	−0.3	[4]

Oxygen and boron were analyzed in Refs. [1,4].

Table 5
Neodymium, praseodymium, cobalt, iron and boron contents analyzed by EDX + WDX or by EDX for the TM-rich phase (or α-TM)

Alloy or Magnet composition (at%)	Measured concentration (at%)			Ref.
	RE	TM	B	
$Nd_{12.8}Fe_{79.8}B_{7.4}$ magnet	<1	99.5	—	[16]
$Nd_{13.7}(Fe_{63.5}Co_{16.7})B_6Zr_{0.1}$ alloy	<1	100.0	—	[9]
$Pr_{13.7}(Fe_{63.5}Co_{16.7})B_6Zr_{0.1}$ alloy	<1	100.0	—	[9]
$Pr_{13.7}(Fe_{63.5}Co_{16.7})B_6Nb_{0.1}$ alloy	1.3	98.7	—	This work
$(Pr_{12.7}Dy_1)(Fe_{63.5}Co_{16.7})B_6Nb_{0.1}$ alloy	1	99.0	—	This work
$Pr_{13.8}(Fe_{63.5}Co_{16.7})B_6$ alloy	<1	99.7	—	This work
$(Nd_{14.4}Dy_{1.6})(Fe_{67}Co_5V_4)B_8$ alloy	<1	99.7	—	[8]
$Nd_{17}Fe_{76.5}B_5Cu_{1.5}$ magnet	4.5	94.8	—	This work
$Pr_{17}Fe_{76.5}B_5Cu_{1.5}$ alloy 1	<1	99.2	<1	This work
$Pr_{17}Fe_{76.5}B_5Cu_{1.5}$-annealed alloy 1	<1	99.1	<1	This work
$Pr_{17}Fe_{76.5}B_5Cu_{1.5}$ alloy 2	<1	99.3	<1	This work
$Pr_{17}Fe_{76.5}B_5Cu_{1.5}$-annealed alloy 2	<1	99.4	<1	This work
$Pr_{20}Fe_{74}B_4Cu_2$ alloy	5.5	91.4	3.1	This work

Zirconium was analyzed in Ref. [9] (<1 at%).
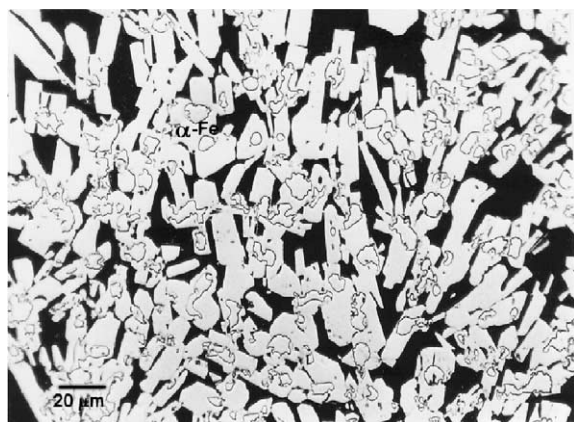
Fig. 9. Micrograph showing free iron on a $Pr_{20}Fe_{74}B_4Cu_2$ alloy (etched with nital).

Ref. [1]. Deviation from stoichiometry is of great magnitude in this case since there is a greater amount of boron in this phase. Measured concentration of RE and TM is nearly twofold the correct value, but identification is quite straightforward. Fig. 8 shows that the RE content on the boride, measured by EDX is 22.4 at%, almost twice the stoichiometric value of 12.1 at%.

Due to the peritectic nature of RE–TM–B alloys, a TM-rich phase can be found inside the matrix phase (see for example Ref. [23]). Measured compositions for this phase are listed in Table 5, and Fig. 9 shows a typical micrograph of an alloy containing this phase. Another TM-rich phase containing a higher amount of RE can be found in alloys with boron content below stoichiometry (5.9 at%). Table 6 gives the measured composition for this RE_2TM_{17} phase and its identification is shown in Fig. 10. Although its composition is similar to that of the matrix phase (EDX) it is easily recognized by the different contrast. Since backscattered electron image reveals the difference between the average atomic numbers of the phases, the differences in contrast show that the phases have different compositions [19].

4. Conclusions

The relative atomic ratio TM:RE used as an indicator of the matrix phase in analyses of alloys and permanent magnets carried out using energy-dispersive X-ray spectrometry varies considerably. In spite of that, it has been shown that the matrix phase can be identified using this ratio. In analyses using a combination of EDX and WDX this ratio varies considerably less. It has been shown that the analyses of RE-rich, TM-rich, B-rich and RE_2TM_{17} phases by EDX is straightforward. The

Table 6
Neodymium, praseodymium, iron and copper contents analyzed by EDX for the RE_2TM_{17} phase

Alloy or magnet composition (at%)	Measured concentration (at%)			TM:RE ratio	Ref.
	RE	TM	Cu		
$Nd_{17}Fe_{76.5}B_5Cu_{1.5}$ magnet	11.1	88.9	0.0	8.0	[2]
$Pr_{20}Fe_{74}B_4Cu_2$ magnet 1	14.3	85.6	<1	6.0	This work
$Pr_{20}Fe_{74}B_4Cu_2$ magnet 2	13.4	86.3	<1	6.5	This work
$Pr_{20}Fe_{74}B_4Cu_2$ heat-treated magnet 1	12.5	87.5	<1	7.0	This work
$Pr_{20}Fe_{74}B_4Cu_2$ heat-treated magnet 2	12.7	87.3	<1	6.9	This work

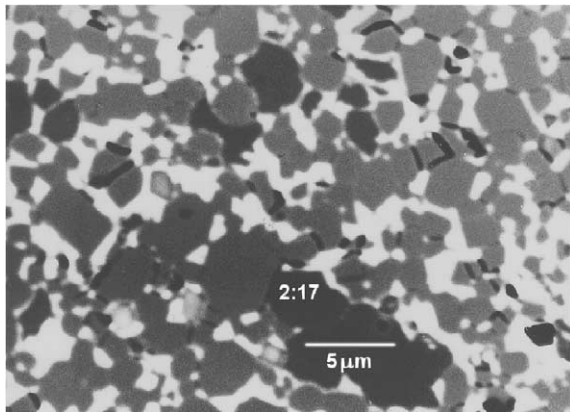Boron was analyzed by WDX in Ref. [2].

Fig. 10. Backscattered electron image showing the 2:17 phase ($Pr_{20}Fe_{74}B_4Cu_2$ magnet).

EDX-measured composition of the RE_2TM_{17} phase is similar to that of the matrix phase.

Acknowledgements

References

[1] X.J. Yin, M.G. Hall, I.P. Jones, R.N. Faria, I.R. Harris, J. Magn. Magn. Mater. 125 (1993) 78.

[2] A. Kianvash, I.R. Harris, J. Alloys Compounds 178 (1992) 325.

[3] F.M. Ahmed, D.S. Edgley, I.R. Harris, J. Alloys Compounds 209 (1994) 363.

[4] D.S. Edgley, J.M. Le Breton, S. Steyaert, F.M. Ahmed, I.R. Harris, J. Teillet, J. Magn. Magn. Mater. 173 (1997) 29.

[5] J.C.S. Onelli, A. Tschiptschin, F.J. Landgraf, Eighth Symposium on Magnetic Anisotropy and Coercivity in RE-TM Alloys, Birmingham, UK, 1994, p. 261.

[6] J. Jiang, Z. Zeng, J. Wu, M. Tokunaga, J. Magn. Magn. Mater. 214 (2000) 61.

[7] R.S. Mottram, A.J. Williams, I.R. Harris, J. Magn. Magn. Mater. 217 (2000) 27.

[8] X.J. Yin, I.P. Jones, I.R. Harris, J. Magn. Magn. Mater. 116 (1992) L325.

[9] R.N. Faria, B.E. Davies, D.N. Brown, I.R. Harris, J. Magn. Magn. Mater. 296 (2000) 223.

[10] H. Yamamoto, S. Hirosawa, S. Fujimura, K. Tokuhara, H. Nagata, M. Sagawa, IEEE Trans. Magn. MAG-23 (5) (1987) 2100.

[11] C. Koestler, R. Ramesh, C.J. Echer, G. Thomas, J. Wecker, Acta Metall. 37 (7) (1989) 1945.

[12] S. Arai, T. Shibata, N. Koshizuka, M. Nagakura, IEEE Trans. Magn. MAG-23 (5) (1987) 2299.

[13] T. Mizoguchi, I. Sakai, H. Niu, K. Inomata, IEEE Trans. Magn. MAG-23 (5) (1987) 2281.

[14] C. Koestler, M. Chandramouli, G. Thomas, L. Schultz, J. Magn. Magn. Mater. 110 (1992) 264.

[15] R.S. Mottram, A.J. Williams, I.R. Harris, J. Magn. Magn. Mater. 222 (2000) 305.

[16] H.R.M. Hosseini, A. Kianvash, M.S. Reihani, H.Y. Zadeh, J. Alloys Compounds 298 (2000) 319.

[17] K.W. Dennis, F.C. Laabs, B.A. Cook, J.L. Harringa, A.M. Russell, R.W. McCallum, J. Magn. Magn. Mater. 231 (2001) L33.

[18] J. Fidler, IEEE Trans. Magn. MAG-23 (5) (1987) 2106.

[19] R.N. Faria, X.J. Yin, J.S. Abell, I.R. Harris, J. Magn. Magn. Mater. 129 (1994) 263.

[20] P.V.P. Marcondes, R.N. Faria, Mater. Sci. Eng. A 272 (1999) 245.

[21] R. Fruchart, R. Madar, A. Rouault, Ph. L'Héritier, P. Taunier, D. Boursier, D. Fruchart, P. Chaudouet, 1984, Institut National de la Propriété Industrielle (Paris) déposé le 9 juin 1984, No. 84 10387, European Patent Office (The Hague, The Netherlands), 20 June, 1985, No. 85 401230.9 (Applicant: CNRS), US Patent and Trademark Office, Washington, DC, Filed June 19, 1985, serial No. 746, 360.

[22] I.R. Harris, J. Less-Common Met. 131 (1987) 245.

[23] A. Kianvash, I.R. Harris, J. Alloys Compounds 279 (1998) 245.